Global Biogeochemical Cycles

RESEARCH ARTICLE
10.1029/2023GB007828

The Importance of Riverine Nutrient Supply for the Marine Silica Pump of Arctic Shelves: Evidence From the Laptev Sea

M. C. F. Debyser[1,2], L. Pichevin[1], R. E. Tuerena[3], A. Doncila[1], I. Semiletov[4,5], and R. S. Ganeshram[1]

[1]School of Geosciences, University of Edinburgh, Edinburgh, UK, [2]Woods Hole Oceanographic Institution, Woods Hole, MA, USA, [3]Scottish Association for Marine Science, Oban, UK, [4]Far East Division of the Russian Academy of Science, V. I. Il'ichev Pacific Oceanological Institute (POI), Vladivostok, Russia, [5]Tomsk State University, Tomsk, Russia

Key Points:

- Rivers supply a large load of dissolved silicon to Eurasian Arctic shelves, where a significant proportion of it is removed through biological activity
- The Laptev Sea is strongly depleted of nitrogen. Differential recycling of dissolved silicon and nitrogen enables additional Si uptake by phytoplanktons and subsequent burial in the sediments
- Biogeochemical cycling processes in the Laptev Sea are traced into the Transpolar Drift. An updated isotopic mass balance budget of the Arctic Ocean illustrates that Arctic shelves significantly contribute to Arctic Ocean's Si cycle and its heavy isotopic enrichment

Supporting Information:

Supporting Information may be found in the online version of this article.

Correspondence to:

M. C. F. Debyser,
margot.debyser@whoi.edu

Citation:

Debyser, M. C. F., Pichevin, L., Tuerena, R. E., Doncila, A., Semiletov, I., & Ganeshram, R. S. (2024). The importance of riverine nutrient supply for the marine silica pump of Arctic shelves: Evidence from the Laptev Sea. *Global Biogeochemical Cycles*, *38*, e2023GB007828. https://doi.org/10.1029/2023GB007828

Received 4 MAY 2023
Accepted 12 MAR 2024

Author Contributions:

Conceptualization: M. C. F. Debyser, L. Pichevin, R. E. Tuerena, A. Doncila, R. S. Ganeshram
Data curation: I. Semiletov
Formal analysis: M. C. F. Debyser
Funding acquisition: I. Semiletov, R. S. Ganeshram
Investigation: A. Doncila, R. S. Ganeshram

Abstract Arctic shelves receive a large load of nutrients from Arctic rivers, which play a major role in the biogeochemical cycles of the Arctic Ocean. In this study, we present measurements of dissolved silicon isotopes ($\delta^{30}Si(OH)_4$) around the Laptev Sea and surface waters of the Eurasian shelves collected in October 2018 to document terrestrial silicon modifications on shelves and their contribution to the Arctic basin. Nitrogen was found to be depleted in surface waters and the limiting nutrient to primary production in the Laptev Sea, allowing excess silicon export to the central Arctic Ocean. Heavy $\delta^{30}Si(OH)_4$ in the water column was linked to the strong biological removal of DSi on shelves, enabled by vigorous N recycling. From isotopically constrained processes, we estimate that >50% of the silicon from riverine inputs is removed within the Lena River delta and on the Laptev Sea shelf. Extrapolating this to major Siberian rivers, this leads to an export of 2.5 ± 0.8 kmol/s of riverine silicon through the Transpolar Drift. An updated isotopic budget of the Arctic Ocean reproduces the observed $\delta^{30}Si(OH)_4$ signatures out of the Arctic Ocean and underlines the importance of biological processes in modulating silicon export. Given that opal burial fluxes on Artic shelves are controlled by denitrification and N-limitation, these processes are sensitive to ongoing climate change. As a consequence of higher riverine DSi inputs and shelf denitrification responding to productivity, it is inferred that silicon export from the Arctic Ocean could increase in the future, accompanied by lighter $\delta^{30}Si(OH)_4$ signatures.

Plain Language Summary This study focuses on key nutrients for algal production in areas of high biological importance around the Arctic Ocean: the Eurasian shelves and particularly the Laptev Sea. We show that major Siberian rivers provide large amounts of silicon to the surrounding shallow seas, which is required by diatoms for growth. These shallow Arctic seas are depleted in nitrate and this limits the consumption of available silicon by algae, regulating the sequestration of silicon and carbon in shelf sediments. This currently allows an important fraction of riverine silicon to escape to the central Arctic Ocean. Climate change will lead to increasing freshwater and nutrient loads from Siberian rivers, and modify biological cycles on the shallow Arctic sea shelves. We can therefore expect increases in the output of silicon to the central Arctic Ocean and export to the Atlantic, with far-reaching impacts on productivity and ecology.

1. Introduction

The Arctic Ocean is a shelf sea and is also the ocean which receives the highest input of freshwater and organic matter relative to its volume globally (Dittmar & Kattner, 2003). Shallow shelves primarily ranging between 0 and 50 m depth cover >50% of its total area (Jakobsson, 2002). It represents around 1% of the volume of the world's oceans, yet receives >10% of global riverine discharge (Aagaard & Carmack, 1989; McClelland et al., 2012), which supplies essential terrestrial material to the Arctic Ocean. Nitrate and dissolved silicon (DSi) are key inorganic nutrients required for diatoms, which are important primary producers in polar ecosystems, contributing to around 50% of primary production in the Arctic Ocean (Krause et al., 2019; Sakshaug, 2004). Around three quarters of the primary productivity of the Arctic Ocean occurs on Arctic shelves, which also account for >90% of opal production (Macdonald et al., 2010). This makes nutrient cycling in shelf ecosystems disproportionately important for regulating the export of inorganic nutrients to the central Arctic Ocean and the North Atlantic.

The Eurasian margin constitutes half of the Arctic Ocean's total shelf area (Jakobsson, 2002), and is important to the silicon budget of the Arctic Ocean. While riverine influence is relatively low (200 km^3/yr) on the extensive Barents Sea (BS) shelf, the Kara, Laptev, and East Siberian Seas receive freshwater input from four major rivers,

Methodology: M. C. F. Debyser, L. Pichevin, R. S. Ganeshram
Project administration: I. Semiletov, R. S. Ganeshram
Resources: I. Semiletov
Supervision: L. Pichevin, R. E. Tuerena, R. S. Ganeshram
Validation: R. E. Tuerena, R. S. Ganeshram
Visualization: M. C. F. Debyser
Writing – original draft: M. C. F. Debyser
Writing – review & editing: M. C. F. Debyser, L. Pichevin, R. E. Tuerena, A. Doncila, I. Semiletov, R. S. Ganeshram

the Ob, Yenisey, Lena, and Kolyma rivers, which contribute to >1,700 km^3/yr of freshwater to the surrounding shallow shelf seas. These major rivers provide large supplies of carbon and DSi to the Arctic Ocean (Holmes et al., 2012; Laukert et al., 2022). On the Laptev Sea shelf, diatoms are the predominant form of marine primary producers and support a large settling flux of organic carbon and nutrients to the seafloor (Cremer, 1999; Fahl et al., 1999).

Stable isotope measurements of DSi, $\delta^{30}Si(OH)_4$, provide useful insights into DSi sources, drawdown and export to surface waters within the Arctic Ocean (Brzezinski et al., 2021; Liguori et al., 2021; Varela et al., 2016). Previous Si budgets and isotopic mass balance for the Arctic Ocean have struggled to reconcile the net export of silicon from the Arctic to the Atlantic Ocean (Torres-Valdés et al., 2013) with the heavy $\delta^{30}Si(OH)_4$ of polar waters compared to the global ocean (Brzezinski et al., 2021; Debyser et al., 2022; Giesbrecht et al., 2022; Liguori et al., 2020, 2021; Varela et al., 2016). A hypothesis to reconcile this discrepancy is the partial utilization of terrestrial DSi and implies burial of isotopically light opal over Arctic shelves (Brzezinski et al., 2021; Debyser et al., 2022; Laukert et al., 2022). This mechanism can explain the export of residual DSi and with heavy $\delta^{30}Si(OH)_4$ after isotopically light Arctic riverine sources of DSi (Mavromatis et al., 2016; Pokrovsky et al., 2013; Sun et al., 2018) are fractionated by diatom uptake (De La Rocha et al., 2000). However, such fractionation also requires both large-scale burial of silicon in the shallow shelves and large terrestrial DSi inputs to close the Arctic Si budget (Laukert et al., 2022). Such processes remain to be documented and quantified in situ.

Understanding the removal of DSi over Eurasian shelves and near major river deltas is important as it ultimately controls DSi fluxes and cycling in the central Arctic Ocean through its transport via the Transpolar Drift (TPD, Charette et al., 2020; Liguori et al., 2021), and its net export to the North Atlantic. This study aims to document and quantify silicon fluxes in the Eurasian shelf to delineate riverine inputs, biological uptake and regeneration and potential burial through the use of $\delta^{30}Si(OH)_4$. Additionally, we aim to understand the controls on DSi export to the central Arctic through the TPD and elucidate how future climate change may affect this. In this study, we present full depth profiles of $\delta^{30}Si(OH)_4$ along a transect in the Laptev Sea, as well as surface measurements from the Eurasian shelves. This, combined with hydrographic data, allows us to examine the importance of riverine nutrient supply in the Arctic Ocean to evaluate the role of "Arctic shelf silica pump," and develop an isotope constrained budget of Si in the Arctic Ocean.

2. Materials and Methods

2.1. Study Area

Samples were collected in October 2018 during the 73rd expedition of R/V *Akademik Mstislav Keldysh* (AMK73). The main transect is located in the Laptev Sea along the Lena estuary, shelf area and the upper part of the continental slope. Underway samples were also collected during transit covering the Eurasian shelf (see Figure 1). The stations were free of sea ice at the time of sampling.

On Eurasian shelves, the surface waters of the BS are dominated by warm, saline Atlantic Waters (AW) inflowing from the North Atlantic through the BS Opening (Årthun et al., 2011; Rudels et al., 2004). The discharge from major rivers forms freshwater plumes and freshened surface layers over wide areas of the Kara and Laptev seas (Spivak et al., 2021), leading to buoyant, eastward-traveling boundary currents (Osadchiev et al., 2020; Semiletov et al., 2005). Much of this plume enters the TPD within 1–2 years and reaches the Fram Strait in 2–3 years (Semiletov et al., 2000), undergoing periodic mixing with underlying AW and vigorous cycling of nutrients on the shelves prior to transport (Thibodeau et al., 2017), before eventually being exported to the North Atlantic through the TPD (Karcher & Oberhuber, 2002) along with terrigenous nutrients (Charette et al., 2020).

The Laptev Sea receives discharge from one of the largest rivers on earth, the Lena River, which supplies large amounts of organic and inorganic nutrients to the surrounding shelf (Holmes et al., 2012; Stedmon et al., 2011). Because of the influence of the Lena River, the hydrography of the Laptev Sea is characterized by large gradients in physical and chemical properties within the water column (Kostyleva et al., 2020; Spivak et al., 2021). As discharge from the Lena River enters the sea, the Lena Freshwater Plume (LFP) is formed. The buoyant fresh water mass at the surface of the water column overlies saline waters, setting up a strong salinity gradient which restricts mixing. These shelf waters gradually become more saline as they extend out toward the continental slope where they meet the inflow of AW via the Norwegian Sea. The discharge of the Lena River varies strongly with

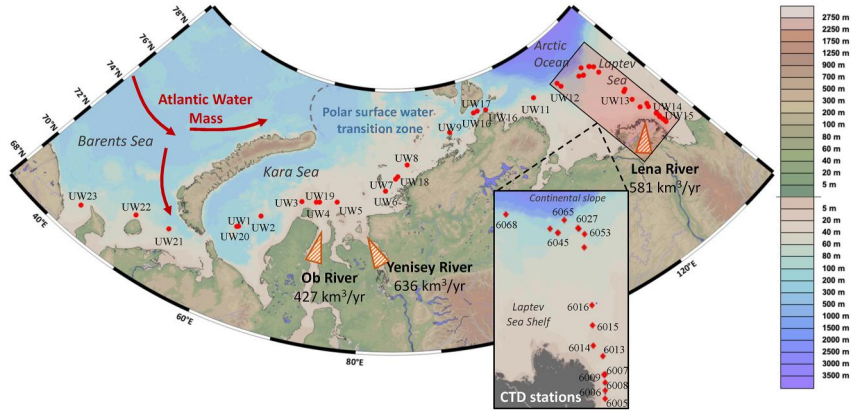

Figure 1. Map showing the study area of this research and general surface circulation patterns of the Eurasian shelves. Red arrows represent warm, saline current of Atlantic water. Orange triangles show the delta of major rivers within the study area, which constitute the largest freshwater source to the Eurasian Arctic sector: the Ob, the Yenisey and the Lena rivers. Discharge is in km^3/yr. AMK73 CTD and underway sample locations are shown with red dots. Shaded red area highlights the CTD section. Station numbers are labeled UW for underway samples and numbered for CTD stations. Map modified from Ocean Data View.

seasonality as the lower reaches of the catchment freeze in winter contracting the extent of the plume on the shelf, and subsequently expands in spring-summer as the Lena discharge increases (Kostyleva et al., 2020; Pavlov et al., 1996). Variations from the Lena discharge also affect the chemical and physical properties of the Lena plume in the Laptev Sea. Underneath the plume, near-bottom stagnant waters are found, constrained by local bathymetry (Kostyleva et al., 2020; Létolle et al., 1993).

2.2. Physical Parameters

Seawater samples were collected from rosette-mounted Niskin bottles equipped with sensors recording physical parameters (conductivity, temperature, pressure and salinity). The relative fraction of freshwater (F_{FW}) in a sample was calculated as follows:

$$F_{FW} = 1 - (S_{obs} / S_{mar})$$

where S_{obs} is the measured salinity of a given sample, and $S_{mar} = 34.92$ psu (Bauch et al., 2010). While we recognize that the oxygen isotope of seawater ($\delta^{18}O$-H_2O) can provide valuable distinction between riverine and sea-ice melt components of freshwater in the Laptev Sea (Bauch et al., 1995, 2010; Laukert et al., 2022), this data set was not available for AMK73 at the time of publication.

2.3. Dissolved Nutrient Concentrations

Dissolved inorganic nutrient concentrations were determined onboard using an autoanalyzer following standard colorimetric methods. The underway samples were immediately frozen on collection and subsequently analyzed for nutrient concentrations at the Scottish Association for Marine Science using a Shimadzu TOC-V analyzer and reference materials from the University of Miami (Hansell lab) were run within each batch. The detection limits for nutrient analysis was 0.1 and 0.03 μM for DSi and NO_x (=NO_3^- + NO_2^-) respectively. The tracers N* and Si* were calculated from inorganic nutrient concentrations where $N^* = NO_x - PO_4^- * 16$, adapted from Gruber and Sarmiento (1997), and $Si^* = SiOH_4 - NO_x$ (Sarmiento et al., 2004). Both tracers are indicative of deviation from typical Redfield ratio and average DSi:N ratios of marine dissolved nutrient ratios, respectively (DSi:N is defined here as DSi:NO_x).

2.4. Silicon Isotopes

250 ml water samples were collected from Niskin bottles onboard and from the ship's underway system and filtered inline using Nuclepore polycarbonate membranes (0.4 μm pore size). The water samples were immediately acidified with 0.1% v/v 12 M HCl for preservation and stored at 4°C until analysis. $\delta^{30}Si$ was determined

following the protocol described in Debyser et al. (2022) for low concentration determination (<10 μM), following the Magnesium Induced Coprecipitation method described in Karl and Tien (1992), Brzezinski et al. (2003), and Reynolds et al. (2006), using volumes of 40 ml of seawater for precipitation as per Debyser et al. (2022).

Resulting solutions were analyzed on a Nu Plasma II MC-ICP-MS at the University of Edinburgh using a standard-sample bracketing protocol (Georg et al., 2006) and the primary isotopic standard NBS28. The internal instrumental error is calculated from standard-sample bracketing during an individual analytical session. Following corrections in Debyser et al. (2022), $\delta^{29}Si$ was converted to $\delta^{30}Si$ using a theoretical conversion factor of 1.96, as calculated from the kinetic fractionation law (Young et al., 2002). This correction was applied to avoid interference on $\delta^{30}Si$ measurements from the low concentrations (Fripiat, Cavagna, Dehairs et al., 2011; Fripiat, Cavagna, Savoye, et al., 2011; Liguori et al., 2021).

The international solid standard Big Batch and both high and low concentration seawater standards $Aloha_{1000}$ and $Aloha_{300}$ were used as reference materials for measurement precision and method reproducibility at low concentrations. Standards were measured with each sample batch. Average standard measurements for the period of this study are: BigBatch = −5.35‰ ± 0.04‰ (n = 8), $Aloha_{1000}$ = +0.63‰ ± 0.05‰ (n = 8) and $Aloha_{300}$ = +0.84‰ ± 0.02‰ (n = 7) for $\delta^{29}Si(OH)_4$, with converted $\delta^{30}Si(OH)_4$ as follow: BigBatch = −10.51‰ ± 0.08‰, $Aloha_{1000}$ = 1.25‰ ± 0.10‰ and $Aloha_{300}$ = +1.66‰ ± 0.05‰, producing an estimated long-term reproducibility of ±0.10‰ for $\delta^{30}Si(OH)_4$. All $\delta^{30}Si(OH)_4$ uncertainties reported in S3 are for 1 SD of the long-term reproducibility unless the internal instrumental error is larger. The measurements of the standard reference material is within ±0.05‰ of $\delta^{30}Si(OH)_4$ from inter-laboratory measurements of BigBatch = −10.48‰ ± 0.2‰, $Aloha_{1000}$ = +1.25‰ ± 0.2‰, $Aloha_{300}$ = +1.66‰ ± 0.35‰ (Grasse et al., 2017; Reynolds et al., 2007).

3. Results

3.1. Eurasian Shelf Transect

Displayed on Figure 2 is the freshwater fraction of surface shelf waters, which increases from West to East (from <5% in the BS to 20%–40% in the Laptev Sea). This illustrates the freshening of eastward-traveling surface boundary currents (Osadchiev et al., 2020) as they gradually pick up riverine discharge. Along the Ob and Yenisey river mouth, riverine fractions reach >60%, and >80% near the Lena Delta, indicative of the riverine freshwater plumes resulting from major Siberian rivers in the Kara and Laptev Sea (Spivak et al., 2021).

Peaks in DSi are observed at the inflows of the Ob and Yenisey (>20 μM) and the Lena Delta (>30 μM), with a general increase in DSi from West to East, with concentrations of ∼5 μM in the BS increasing to >10 μM in the East Kara Sea and the Laptev Sea, showing riverine discharge is increasing the DSi content as well as modifying nutrient stoichiometry of surface shelf waters from DSi:N <10 to >15.

Positive $\delta^{30}Si(OH)_4$ are measured and range from +0.74‰ to +2.41‰ across the transect. The isotopically lowest measurements are found in the Lena Delta plume in samples that have the highest freshwater fraction (+0.74‰ to +1.44‰), which aligns well with estimates of +0.86‰ ± 0.3‰ from Sun et al. (2018) for the average signature of the annual Lena Delta $\delta^{30}Si(OH)_4$ influx and summer $\delta^{30}Si(OH)_4$ measured in the Laptev Sea. Lighter $\delta^{30}Si(OH)_4$ are also measured in the Ob and Yenisey plume (+1.78‰ to +1.95‰), in agreement with findings in Mavromatis et al. (2016) that the $\delta^{30}Si(OH)_4$ of the Yenisey is isotopically heavier than other Eurasian rivers due to deep underground flow through permafrost. Away from the freshwater plumes, a general increase in $\delta^{30}Si(OH)_4$ is observed from lower longitudes of the East Kara Sea to the East of the Laptev Sea, increasing from ∼+1.8‰ to ∼+2.4‰ while DSi concentrations remain ∼12 μM.

3.2. Laptev Sea Transect

3.2.1. Hydrographic Structure

As shown in Figure 3, large salinity and temperature gradients are observed in the estuarine region across the Lena delta and the continental slope of the Laptev Sea. Salinity varies from <10 psu in the upper 10 m of the water column near the Lena Delta to >34 psu over the continental slope. Temperatures vary from 2 to 5°C around the Lena Delta to 1°C in the upper 30 m of the continental slope, overlying cold (−1°C), saline waters.

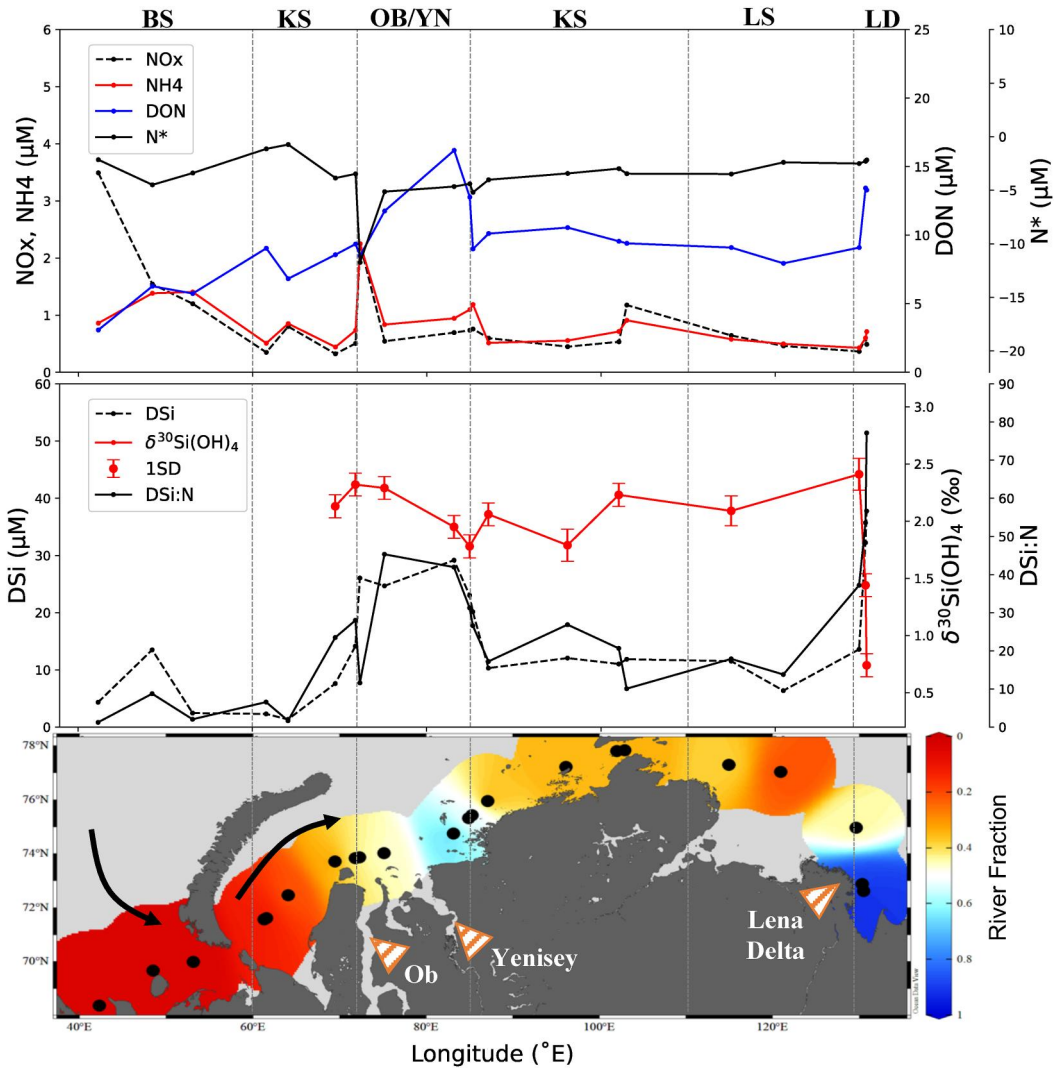

Figure 2. Longitudinal transect of nutrient concentrations and isotopic measurements of underway samples of AMK73. Top panel: Dotted black lines display surface concentrations of NO_x (nitrate + nitrite, µM) concentrations, red line is ammonia (µM), blue line is dissolved organic nitrogen (µM), and black line is N* (=NO_x − 16 * PO_4, µM) with longitude along the Eurasian shelf. Middle panel: Displayed are surface concentrations of DSi (black dotted line, µM), $\delta^{30}Si(OH)_4$ (red line, ‰) and DSi:N (black line) with longitude along the Eurasian shelf. Bottom panel: Calculated freshwater contribution to underway measurements along the transect. BS = Barents Sea, KS = Kara Sea, OB/YN = Ob and Yenisey river inflow, LS = Laptev Sea, LD = Lena Delta inflows.

The fresh, colder plume of water in the upper 15 m of the Lena Delta region (at latitudes of 72.5°–74.5°) characterizes the core of LFP. During the expedition of AMK73 in October 2018, this extends out northward and contributes to a Surface Freshwater Layer (SFL) in the upper 20 m of the water column, overriding denser, more saline advected and modified AW. Under the LFP, colder, more saline (<1°C, >25 psu) waters are found, characteristic of older shelf waters constrained locally by hydrography (Kostyleva et al., 2020; Létolle et al., 1993). The LFP and SFL are strongly stratified in the summer months from the surrounding waters by steep salinity gradients, restricting the exchange of nutrients, before mixing in the winter (Janout et al., 2020). LFP is the least saline with >70% freshwater. The influence of riverine freshwater decreases in the SFL but is still high, with a freshwater content between 20% and 50%. Old Shelf Waters (OSW) have >30% freshwater content, indicating a strong influence from the overlying river plume.

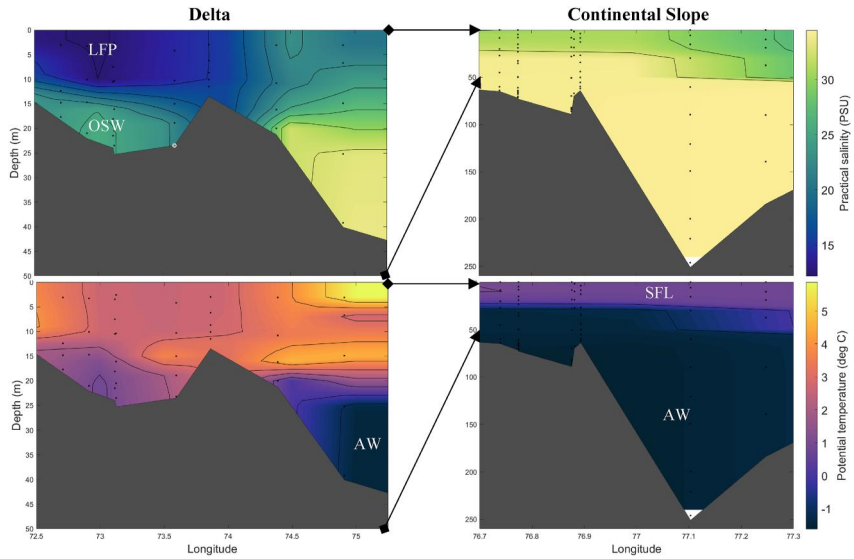

Figure 3. Hydrography of the Laptev Sea in October 2018 along the CTD transect of AMK73. Left panels: Lena Delta. Right panels: Laptev shelf and continental slope. Top panels show salinity and bottom panels show temperature (°C). LFP = Lena Freshwater Plume, OSW = Old Shelf Water, AW = Advected Atlantic Water, SFL = Surface Freshwater Layer.

3.2.2. Nitrogen Concentrations and Distribution

Figure 4 displays the distribution of NO_x, dissolved organic nitrogen (DON) and N* across the Laptev shelf. Overall, nutrient distribution largely follows the major hydrographic structure of the transect. In the LFP, NO_x is depleted (<1 μM), but DON concentrations are high (>10 μM), confirming that nitrogen supplied by the Lena river is mostly in organic form in the summer (Holmes et al., 2012; Thibodeau et al., 2017). DON concentrations rapidly decrease in the SFL, while NO_x remains low. In the advecting AW, NO_x concentrations are high (>10 μM). In the OSW, NO_x varies locally but generally the concentrations are higher near the bottom, potentially

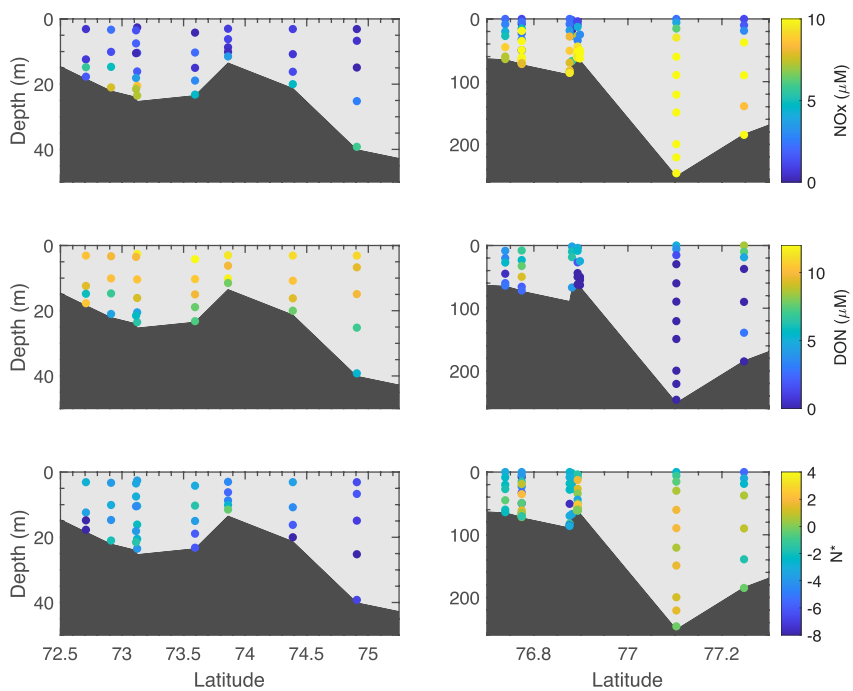

Figure 4. NO_x (μM, top panels), dissolved organic nitrogen (μM, middle panels), and N* (=NO_3 − 16 * PO_4, μM, Gruber & Sarmiento, 1997, bottom panels) along the Lena Delta (left panels) and over the continental slope (right panels) for AMK73.

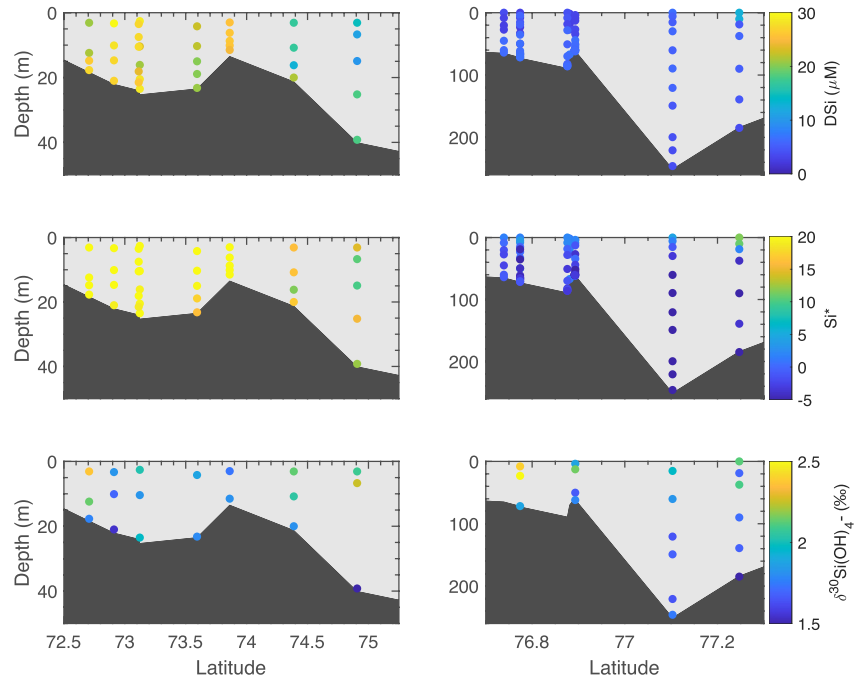

Figure 5. DSi (top panels), Si* (=DSi − NO_3, μM, middle panels) and $\delta^{30}Si(OH)_4$ (bottom panels) along the Lena Delta (left panels) and over the continental slope (right panels) for AMK73.

reflecting benthic remineralization of nitrogen and subsequent sedimentary supply to the water column (Sun et al., 2021). N*, where positive values reflect the relative enrichment of nitrate in comparison to phosphate (Gruber & Sarmiento, 1997), are highly variable over the section (bottom panels of Figure 4). In the LFP and the SFL, N* is negative, indicating low N-availability for uptake with respect to phosphate in freshwater. Combined with the depleted NO_x concentrations observed on the surface, this suggests that primary production on the shelf is N-limited. Negative N* values are observed down to the sediments and decrease offshore of the Lena Delta, indicating that nitrogen deficit is not limited to the euphotic zone. Positive N* is observed in AW advecting over the Laptev Sea shelf, indicative of its relatively N-rich origins, while N* remains negative in the upper fresh water layer of the continental slope.

3.2.3. Silicon Concentrations and Isotope Distribution

DSi concentrations, Si* and the $\delta^{30}Si(OH)_4$ for the Laptev Sea transect are shown in Figure 5. DSi concentrations largely follow salinity trends, with high values (>30 μM) in the LFP, which subsequently decrease in the SFL. This follows previous findings that with exception to OSW, DSi concentrations are well correlated with riverine influence from the Lena River (Kostyleva et al., 2020; Létolle et al., 1993). Over the continental slope, low DSi concentrations are generally observed, reflective of AW poor in DSi owing to its origins in the North Atlantic. A gradient is observed in Si* from South to North along the transect. Positive Si* (>20 μM) are observed close to the Lena Delta, reflecting the high DSi:N stoichiometry of terrestrially supplied nutrients, with values gradually decreasing to reach negative (<0) over the continental slope.

Positive $\delta^{30}Si(OH)_4$ values are measured along the Laptev Sea transect, ranging from +1.43‰ to +2.55‰ (Figure 5). This is within the range of $\delta^{30}Si(OH)_4$ measured in the Laptev Sea in 2013–2014 (+0.91‰ to +3.82‰, Laukert et al., 2022). Measurements of $\delta^{30}Si(OH)_4$ from Laukert et al. (2022) and measurements within this study agree very well at comparable freshwater fractions and DSi concentrations (Figure 7), with regional differences arguably arising from local hydrography and seasonal discharge as well as the extent of utilization by seasonal diatom blooms, all depending on the timings of sampling, which largely dictates $\delta^{30}Si(OH)_4$ distribution. Generally, in our study, isotopically higher values are measured toward the surface in the LFP and SFL, with decreased DSi concentrations, consistent with fractionation from biological uptake by silicifying species (i.e., diatoms) during growth. The average $\delta^{30}Si(OH)_4$ for AW is +1.72‰ ± 0.16‰, which is consistent with

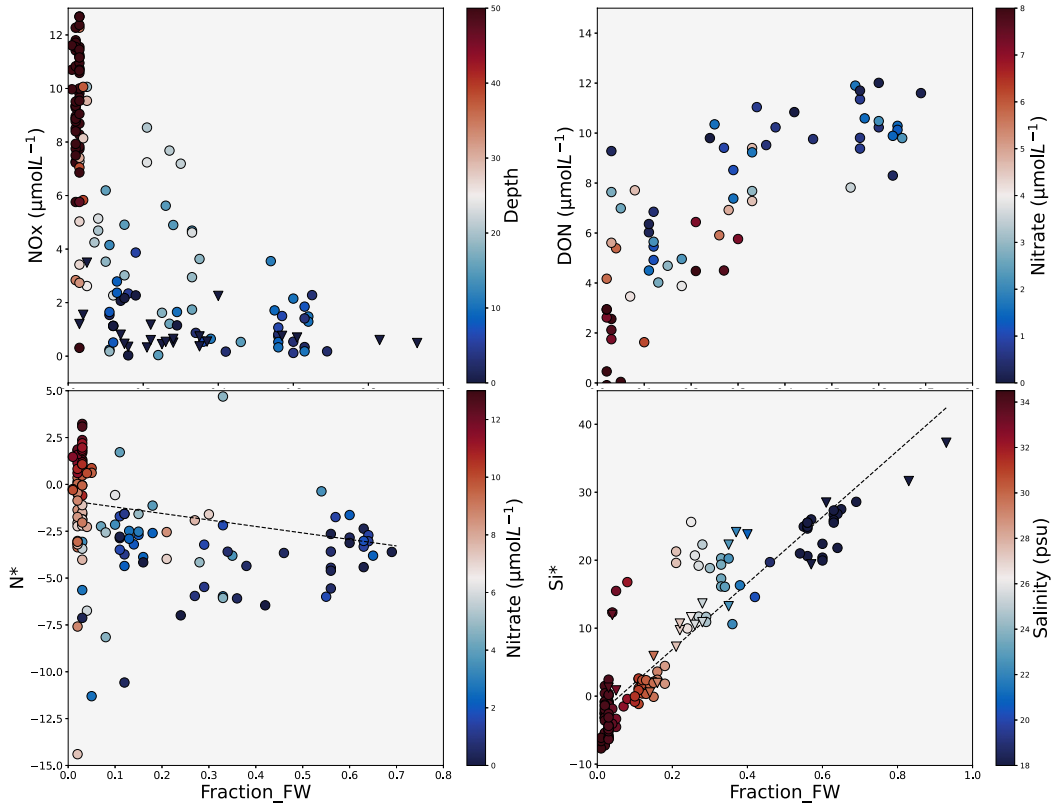

Figure 6. Nitrogen species and their derived parameters with relation to freshwater content (Fraction_FW) of samples on AMK73. Top left: NO_x (µM), color scale is depth (m). Top right: dissolved organic nitrogen (DON, µM), color scale is nitrate (µM). Bottom left: N* (=NO_3 − 16 * PO_4, µM), color scale is nitrate (µM). The dotted black line shows least square regression. Bottom right: Si* (=DSi − NO_3, µM), color scale is salinity (psu). Black line shows least square regression. Circles show measurements from CTD casts and triangles are from the ship's underway system.

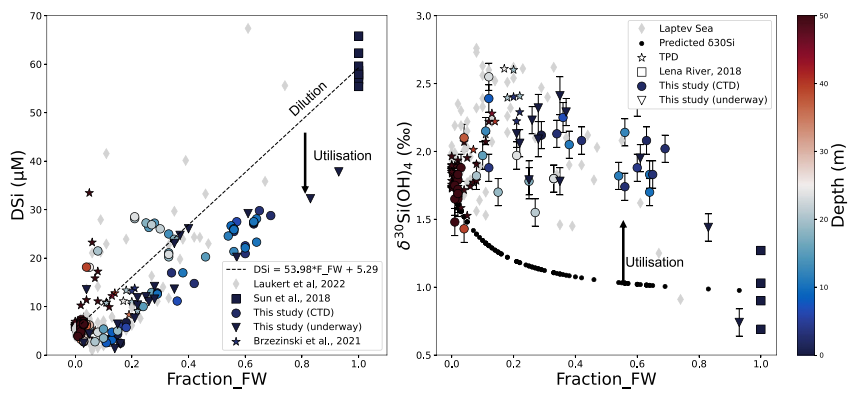

Figure 7. (a) DSi against freshwater fraction (left) and (b) $\delta^{30}Si(OH)_4$ against freshwater fraction (right). Circles show measurements from the CTD casts of this study (AMK73), and triangles are from the ship's underway system. Black squares are measurements from the Lena river (Sun et al., 2018), gray diamonds are from Laukert et al. (2022) in the Laptev Sea for inter-annual and seasonal comparison of $\delta^{30}Si(OH)_4$, and stars are from TPD stations (stations 30, 32, 38, and 43, depths <500 m) in the central Arctic Ocean (Brzezinski et al., 2021). Color scale is depth (m). Dotted lines show the theoretical conservative mixing line between the Atlantic Water endmember (defined here as freshwater fraction <0.1) and the Lena river freshwater endmember at the main river outflow below the three main tributaries (from Sun et al., 2018). The calculation of predicted $\delta^{30}Si(OH)_4$ is described in Section 4.3.

measurements of $\delta^{30}Si(OH)_4$ of AW at Fram Strait (Debyser et al., 2022) and aligns closely with measurements of waters from North Atlantic origin (Brzezinski & Jones, 2015; Souza et al., 2012), confirming that DSi in AW is of Atlantic origin. In the LFP, $\delta^{30}Si(OH)_4$ is variable but generally high (+1.95‰ ± 0.2‰) with high DSi concentrations (25 ± 2 μM), driven by diatom-dominated utilization (Laukert et al., 2022).

4. Discussion

DSi concentrations and nutrient stoichiometry along the Eurasian shelf are strongly linked to the local hydrography and display a particularly strong relationship with freshwater influence (Figures 2, 4, and 5), highlighting the role of Eurasian rivers in modifying freshwater and nutrient budgets of Arctic shelves. Next, we focus on the processes that transform riverine inputs as well as the controls on DSi removal and export to the central Arctic Ocean.

4.1. Transformation of DSi Along the Eurasian Shelf

The $\delta^{30}Si(OH)_4$ signatures of waters from Arctic origin are isotopically heavy. The origins of this enrichment were initially associated with physical mixing processes and biological uptake in the central basins (Liguori et al., 2020; Varela et al., 2016), although recent work points toward the partial utilization of DSi on Arctic shelves instead (Brzezinski et al., 2021; Debyser et al., 2022; Laukert et al., 2022; Liguori et al., 2021). Surface measurements from the Eurasian shelf in this study (Figure 2) show that rivers supply high DSi loads with concentrations peaking near the proximity of rivers but rapidly decreasing away from deltas. We observe a gradual modification Eastward over the Eurasian shelf of $\delta^{30}Si(OH)_4$ in surface waters (+0.6‰) with an increase of ∼1 μM of DSi. Terrestrial sources of DSi to the Arctic Ocean are variable but generally isotopically lighter than marine DSi (+0.4‰ to +1.9‰, Mavromatis et al., 2016; Pokrovsky et al., 2013; Sun et al., 2018) from weathering of bedrock with low $\delta^{30}Si(OH)_4$. While not present at the time of this study, sea ice can also play an important role in vertically redistributing DSi in the water column across seasons (Laukert et al., 2022). Sea ice brine, a potential source of DSi, has a $\delta^{30}Si(OH)_4$ equal or heavier than surrounding waters (Fripiat et al., 2007, 2014) although evidence of this influence in the Arctic Ocean remains limited (Brzezinski et al., 2021; Debyser et al., 2022). The small increase in DSi concentrations coupled with increasing $\delta^{30}Si(OH)_4$ of surface waters reflects the addition of terrestrial DSi coupled with biological consumption of DSi simultaneously occurring on the shallow Eurasian shelves, thereby enriching $\delta^{30}Si(OH)_4$. DSi is only partially utilized as NO_x concentrations are depleted (<1 μM), preventing further biological uptake of DSi and thereby fractionating $\delta^{30}Si(OH)_4$ away from light source values. A significant fraction of biological Si must be sequestered in the sediments for ambient seawater signatures to remain enriched as sedimentary dissolution of biological Si would otherwise return $\delta^{30}Si(OH)_4$ toward source values. A study of porewater nutrient concentrations from Sun et al. (2021) highlights this regionally, with high DSi concentrations in the sediments of the Laptev and East Siberian shelf (100–250 μM) indicating significant sedimentary burial of Si.

In summary, the data show that the high DSi load from riverine sources is removed in the shelf as waters advect, while N concentrations remain low (Figures 2 and 6). In the next section, we explore the cycling processes which can enable substantial DSi removal in N-limited conditions.

4.2. Nitrogen Dynamics in the Laptev Sea

Generally in the Arctic Ocean, primary production is N-limited (Le Fouest et al., 2013; Tuerena, Mahaffey, Henley, et al., 2021). This is exacerbated locally around river mouths by terrestrial inputs of nutrients from Eurasian rivers that have a high DSi:N ratio (Holmes et al., 2012). This input further modifies nutrient stoichiometry and inventories of shelf waters from marine endmembers, leading to a N-deficit with respect to DSi compared to the traditional ratio of ∼1:1 (Brzezinski, 1985; Tuerena, Mahaffey, Henley, et al., 2021). This is seen through the relative increase of DSi:N ratio across the Eurasian shelf on Figure 2 and is also observed in the Lena Delta, where DSi concentrations are high within the LFP and well in excess with respect to N (middle panel of Figure 5). Additionally to high DSi:N terrestrial input, N is also actively removed on Eurasian shelves through processes of sediment denitrification (Chang & Devol, 2009; Fripiat et al., 2018; Le Fouest et al., 2013). Recent work shows substantial benthic N loss due to denitrification in the Laptev Sea (74 mmol $N/m^2/yr$, Sun et al., 2021). Thus, diatom production and biological DSi drawdown are controlled by the availability of N locally

in this region. It also implies that N modulates the proportion of terrestrial DSi which is buried on Eurasian shelves relative to what is exported into the TPD.

Nitrogen from Eurasian rivers is primarily supplied in the form of DON, particularly over the summer months where nitrate represents only 20% of the total DON flux (Holmes et al., 2012). This trend is observed within our study (Figure 4) with high (>10 μM) DON concentrations within the LFP, while nitrate concentrations are low (<2 μM). While DON is not directly available to phytoplankton for uptake, it is quickly cycled to NO_x on the Laptev Sea shelf (62%–76% of DON released from the Lena River is removed within 2 months, Thibodeau et al., 2017). Residence time of waters on Eurasian shelves is estimated to be 1–2 years prior to export through the TPD (Semiletov et al., 2000), and 70% of terrestrial DON is consumed within a couple of years before reaching the marine endmember (Letscher et al., 2013). We observe the conversion of DON to NO_x in the Laptev Sea. For instance, the top panels of Figure 6 show that lower DON at freshwater fractions <0.5 are characterized with higher NO_x, increasing the availability of N for primary production.

Despite this local supply from the conversion of DON, NO_x concentrations in the study area remain very low overall. In the LFP (top panels of Figure 4), NO_x concentrations are depleted (<1 μM), with concentrations varying between 0 and 8 μM over the shelf. As the average nitrate concentration of Eurasian rivers is 4.2 μM (Holmes et al., 2019 from Charette et al., 2020), depletion of NO_x to the concentrations observed in the shelf area imply significant fast removal in the estuary or on the shelf through biological uptake and/or denitrification in freshwater (Francis et al., 2023; Le Fouest et al., 2013; Thibodeau et al., 2017). Supply of additional N through DON cycling appears to be rapidly utilized, with NO_x concentrations quickly returning to near-depletion at higher freshwater fractions (Figure 6). The lack of a linear relationship between NO_x concentrations and N* when plotted against freshwater fraction in the subsurface (Figure 6; Left panels) also confirms that the N-deficit is not governed by dilution but through active N-removal processes, with an excess of terrestrial-originating phosphate exported. As in previous studies, DSi behaves quasi-conservatively when oceanic and riverine waters mix in the coastal zone (Left panel of Figure 6, Létolle et al., 1993). Additionally, excess export of DSi from riverine sources is also observed, as highlighted by the linear trend between Si* and riverine fraction (Figure 6; bottom right panel), with Si* reaching 30 μM.

The DSi:N requirement for diatom consumption on Arctic shelves is estimated to be between 1.8 and 2.1 (Macdonald et al., 2010; Simpson et al., 2008; Tremblay et al., 2008). This is lower than the DSi:N ratio observed along the Eurasian shelves owing to depleted NO_x concentrations (Figure 2). The extremely low NO_x concentrations and higher concentrations of phosphate and DSi confirm that N is the limiting nutrient for primary production, limiting DSi drawdown and modulating its export to the TPD (Debyser et al., 2022).

Significant benthic efflux of nutrients is present on the Laptev shelf. Benthic DSi fluxes for the Laptev Sea were estimated at 15% of the total riverine input, and 29% for NO_x (Sun et al., 2021). This implies that terrestrial NO_x is recycled twice as much as DSi, fueling supplementary DSi utilization from recycled N, which has the potential to increase net opal burial. Evidence for nutrient regeneration is observed locally in the OSW of the section, with increased DSi and NO_x concentrations (Figures 4 and 6) and isotopically lower $\delta^{30}Si(OH)_4$ by ~0.4‰ relative to waters outside the OSW (Figure 5). This could be indicative of sediment dissolution of biogenic and lithogenic Si, as demonstrated by Ward et al. (2022b) in the BS where porewater $\delta^{30}Si$ is isotopically light (−0.51‰ to +1.69‰), which could act to lower near-benthic water $\delta^{30}Si(OH)_4$ locally.

These fluxes illustrate that both water column and sediment N cycling is vigorous on the shallow Laptev sea shelf, where N is recycled at least twice as much as Si (Sun et al., 2021). The differential recycling of N and Si allows additional uptake of DSi by diatoms. Considering the processes of recycling and removal of nutrients illustrated above on Arctic shelves, in the following section we aim to quantify the burial of terrestrial DSi on shelves through isotopic constraints. Later, we evaluate whether the shelf processes characterized in this study allow us to close the gap in the Arctic Ocean's isotope budget.

4.3. Calculating DSi Removal on the Laptev Shelf

We have established that nitrogen is the limiting nutrient to primary productivity in the Laptev Sea and modulates the Si fraction that is removed on Arctic shelves. The data in Figure 7 (left panel) confirms this through the linear trend in DSi concentrations, which is parallel to the AW-freshwater theoretical dilution line. The offset from the dilution line to lower DSi can be explained by biological uptake of nutrients. This uptake is evident in Figure 7

(right panel) through the deviation toward heavier values of $\delta^{30}Si(OH)_4$ from their predicted isotopic mixing signatures (black circles). Figure 7 also shows a comparison of $\delta^{30}Si(OH)_4$ measured in the TPD (Brzezinski et al., 2021). Surface waters of the TPD with high riverine influence (>0.1) meet the trend of increasing $\delta^{30}Si(OH)_4$ with DSi utilized on the Laptev shelf/slope (this study). $\delta^{30}Si(OH)_4$ signatures show mixing between AW-sourced DSi and isotopically enriched DSi sourced from Eurasian rivers and partially utilized on the Eurasian shelves, illustrating that DSi from Eurasian shelves directly feeds into the export of inorganic nutrients to the central Arctic Ocean, namely through the TPD. Findings from Liguori et al. (2021) and Laukert et al. (2022) concur with direct evidence of isotopically heavy Eurasian shelf-derived DSi in the TPD. This establishes that geochemical cycling of nutrients on the Arctic shelves exerts important controls on the export of nutrients to the central Arctic Ocean. Next, we attempt to quantify the proportion of DSi which is removed in the shelf area using $\delta^{30}Si(OH)_4$ and simple mixing models.

In Figure 7 (right panel), we present predicted mixing $\delta^{30}Si(OH)_4$ signatures at freshwater fractions between the Lena river and the Laptev Sea. The predicted $\delta^{30}Si(OH)_4$ assumes changes in isotopic signatures are only controlled by physical mixing between the two endmembers, and no modification via biological processes occurs on the shelf, as described in Text S2 in Supporting Information S1. The endmembers used are AW (DSi = 6.37 ± 3.04 µM, $\delta^{30}Si(OH)_4 = +1.73‰ \pm 0.16‰$; this study) and Lena waters (59.3 ± 3.3 µM, $\delta^{30}Si(OH)_4 = +0.97‰ \pm 0.24‰$, Sun et al., 2018). All measured $\delta^{30}Si(OH)_4$ with a freshwater fraction >0.1 were heavier than predicted $\delta^{30}Si(OH)_4$, enriched by up to 1.3‰. This implies removal of a significant proportion of riverine Si through burial in the shelf sediments, along with the left panel of Figure 7 that shows a net deficit of DSi compared to the theoretical mixing line. This removal of riverine Si on the Laptev shelf can be evaluated using simple fractionation models.

We evaluated the proportion of riverine silicon removal on the Laptev shelf using $\delta^{30}Si(OH)_4$ through closed and open system models of fractionation. The equations and parameters for these models are fully described in Text S2 in Supporting Information S1. As the LFP is strongly salinity stratified, we expect replenishment of nutrients to the surface via mixing with underlying waters to be limited and estimate that closed system fractionation is a good approximation of the physical conditions on the Laptev Sea shelf in late summer 2018.

Using a closed-system model, the estimated mean shelf DSi removal from riverine input along the sector is 55% ± 14%. This is comparable with findings from Charette et al. (2020) who found that 43% of DSi is removed in estuaries or over the shelf prior to transport in the TPD. A concentration-only based assessment underestimates opal burial (35% ± 22%, this study). This suggests that nutrient concentrations alone underestimate siliceous primary productivity on the Laptev Sea Shelf, and highlights the role of recycled NO_x within the water column to sustain further drawdown of DSi. Isotopically based calculations are significantly more accurate compared to deduction from concentration data, and sensitive to $^{30}\varepsilon$ and the type of model used. The estimated removal goes up to 76–77% ± 27% based on an open system or Canadian Arctic $^{30}\varepsilon = -0.59‰$ (Giesbrecht et al., 2022). However, these parameters are less likely to describe the hydrographic conditions of the transect, leading to overestimation of removal of DSi compared to the export observed through the TPD, and are not considered further.

The biological pump of the Laptev Sea sequesters a significant amount of opal (Laukert et al., 2022). On an annual basis, 1.53 kmolSi/s is supplied from the Lena river (Holmes et al., 2012), and assuming 55% ± 14% removal as per above, 0.69 ± 0.21 kmolSi/s is exported to the open sea from the shelf area. As much as 0.23 kmolSi/s is resupplied from sediments through benthic efflux on the Laptev shelf (Sun et al., 2021), leading to fluxes of biological uptake of 1.08 ± 0.21 kmolSi/s and burial of 0.84 ± 0.21 kmolSi/s. This leads to an isotopically constrained estimate of burial of 78% ± 19% of the total opal production in the Laptev Sea into the sediments, as illustrated in Figure 8.

Combined, the four major Eurasian rivers deliver 5.5 kmolSi/s (Holmes et al., 2012). Extrapolating the removal observed on the Laptev Sea shelf to the Eurasian shelf, this would lead to a total terrestrial export of 2.5 ± 0.8 kmolSi/s or 5.8 ± 1.8 kmolSi/s if all pan-Arctic rivers are considered (for a pan-Arctic DSi riverine flux of 12.9 kmolSi/s, taken from Holmes et al., 2012). As we find isotopic evidence that DSi directly feeds into the TPD, we can estimate the proportion of DSi from rivers transported within it. Estimated DSi concentrations in the TPD at 20% meteoric water are 12.5 µmol/L and the transport core rate of the TPD is 0.9 ± 0.4 Sv (Charette et al., 2020). This leads to a total flux of DSi of 11.25 ± 5 kmolSi/s, which indicates that around 78 ± 65% of DSi transported within the TPD is of marine origin. This estimation is likely an underestimate of terrestrial DSi export as it only accounts for the four major Siberian rivers and assumes the same intense biological removal for all riverine input

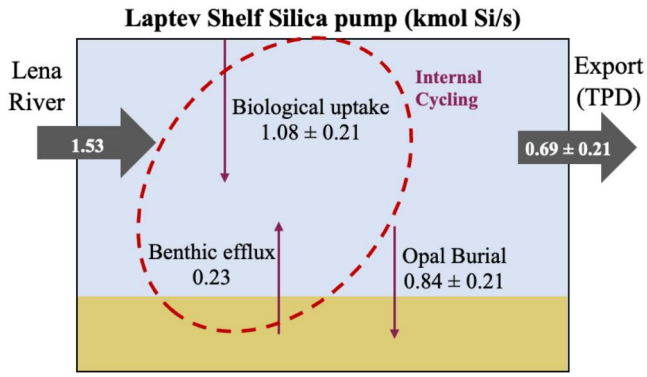

Figure 8. Schematic of the Laptev shelf silica pump with riverine supply of DSi (Holmes et al., 2012), export out of the continental shelf, opal burial, and the internal cycling processes of biological uptake and benthic efflux (Sun et al., 2021). The uncertainty in this simple model is derived from the error in the removal term (±14%), applied to the total riverine DSi flux. In this budget, riverine inputs = export to TPD + opal burial. Inside the dotted red circle shows internal cycling processes. Water column dissolution of opal is assumed to be negligible due to small water column depths (<50 m). All fluxes are shown in kmolSi/s.

on less productive shelves such as the BS. This approximation, however, is of the same magnitude as the export of excess DSi from the Arctic Ocean (15.7 ± 3.2 kmol/s, Torres-Valdes et al., 2013), highlighting the importance of the Siberian rivers in Arctic DSi export, in parallel with findings from Laukert et al. (2022) and Sun et al. (2021).

The use of isotopic tools allows for more accurate determination of DSi export, and highlights the importance of Eurasian rivers as source of DSi to the Arctic Ocean and the importance of shelf cycling in controlling the export of inorganic nutrients. Nonetheless, we observe large variability in the range of DSi export calculated, which is primarily associated with uncertainty in the transport rate of the TPD (standard error is 44% of total rate, Charette et al., 2020), and is sensitive to the annual DSi flux and isotopic signature from rivers.

4.4. Constraining the Arctic Ocean Silicon Isotope Budget

Brzezinski et al. (2021) hypothesized that the burial of isotopically light Si on Arctic shelves is necessary to reproduce the heavy isotopic signature of Arctic outflows and balance the Si isotopic budget of the Arctic (Torres-Valdés et al., 2013). Gaps in the isotopic composition of key gateways such as Fram Strait and the BS Opening increased the overall uncertainty, but recent studies indicate that biological uptake and opal recycling are dominant processes in the DSi budget of the Arctic Ocean (Brzezinski et al., 2021; Laukert et al., 2022), and that shelf production/removal is needed to balance the isotopic budget of the Arctic Ocean.

We use the direct measurements of $\delta^{30}Si(OH)_4$ on the Eurasian shelves presented in this study to update the DSi isotopic mass balance of the Arctic Ocean from Brzezinski et al. (2021) with constraints of biological processes on the Laptev Shelf. The budget also combines the recent data sets describing the $\delta^{30}Si(OH)_4$ of Fram Strait (Debyser et al., 2022), the BS Opening (Debyser, 2023) and recent advances in describing DSi cycling processes (Giesbrecht et al., 2022; Liguori et al., 2020, 2021; Varela et al., 2016; Ward et al., 2022a, 2022b), further described in Table 1.

The DSi budget presented in Table 1 uses the DSi fluxes across Arctic gateways from Torres-Valdés et al. (2013) and pan-Arctic annual riverine DSi fluxes measured over a decade in Holmes et al. (2012) of 0.41 TmolSi/yr, with an additional input of 0.01–0.04 TmolSi/yr from riverine opal leading to a total o.f 0.44 TmolSi/yr, assuming around half of opal material dissolves within the water column (Carey et al., 2020; Tréguer et al., 2021). In the

Table 1
Synthesis of the Silicic Acid and Modeled DSi Isotopic Budget for the Arctic Ocean Compared to Measured $\delta^{30}Si(OH)_4$ Input and Outflux Through the Davis and Fram Straits

		Tmol Si/yr	Range	$\delta^{30}Si(OH)^4$	Range	Isotopic data source
Influx	Bering Strait	0.66[a]		+1.72	1.67–1.77	Giesbrecht et al. (2022), Brzezinski et al. (2021)
	Barents Sea Opening	0.42[a]		+1.67	1.67–1.79	Debyser (2023)
	Fram Strait	0.85[a]		+1.74	1.68–1.80	Debyser et al. (2022)
	Rivers	0.44[b]	0.41–0.45	+1.3	1.00–1.60	Sun et al. (2018)
Observed Input		2.37		+1.64		
Outflux	Davis Strait	−1.35[a]		+1.75		Giesbrecht et al. (2022)
	Fram Strait	−1.08[a]		+1.85	1.76–1.94	Debyser (2023)
Observed Outflux		−2.43		+1.79		
Add. Outputs	Removal—Open	−0.14[c]	−0.18 to −0.10	+1.16	1.16–1.50	Brzezinski et al. (2021)
	Removal—Shelf	−0.24	−0.34 to −0.19	+0.6	0.52–0.72	This study
Modeled Outflux		1.99		+1.80		

Note. This model accounts for additional removal of riverine DSi on Arctic shelves. [a]Torres-Valdes et al. (2013). [b]Holmes et al. (2012). [c]Brzezinski et al. (2021).

Bering Strait, $\delta^{30}Si(OH)_4$ was measured between +1.67‰ and +1.79‰ (Brzezinski et al., 2021; Giesbrecht, 2019), leading to an average of +1.72‰. Fram Strait and the BS opening have inflow signatures of +1.74‰ ± 0.06‰ (Debyser et al., 2022) and +1.67‰ (Debyser, 2023) respectively. Outflowing polar waters have signatures of +1.75‰ (Giesbrecht, 2019) and +1.85‰ ± 0.09‰ (Debyser et al., 2022) for the Davis Strait and Fram Strait, respectively.

Using DSi isotopes, we have evidence that a significant proportion of DSi is removed on the Laptev Sea shelf, implying strong biological control over the DSi budget and significant burial on the shallow Eurasian shelves. There are large associated uncertainties with opal burial. Previous estimates of opal burial for the Arctic Ocean are of 0.16–0.30 TmolSi/yr (Brzezinski et al., 2021; März et al., 2015) based on opal content of 2% weight averaged for the Arctic Ocean. Recently in the BS, opal content was documented to be particularly low (0.26%–0.52% weight), and to be rapidly recycled near the surface of the seafloor (Ward et al., 2022b). Nonetheless, the average of 2% weight can underestimate sedimentary opal content on Eurasian shelves around river deltas, where opal content >3% and up to 13% have been measured in the regions of the Laptev and East Siberian Seas (Mammone, 1998; Nürnberg et al., 1997).

Arctic primary production is highest around coastal areas and is sustained by rivers (Terhaar et al., 2021), and is significantly increasing with climate change (Frey et al., 2021). Most of the Arctic's opal production occurs on shelves, with the Laptev and Kara seas particularly favorable for diatom production (Macdonald et al., 2010). Regional highs in productivity and zones of intense burial may significantly affect exported $\delta^{30}Si(OH)_4$ on a basin-wide scale. Significant differences in nutrient cycling between the BS shelf and other Eurasian shelves may also be observed as the BS Opening experiences strong mixing from tidal and frontal currents, and experiences deep winter convection through its entire water column (Sundfjord et al., 2007), leading to low burial rates of opal in the BS Opening (Ward et al., 2022b). This is not necessarily representative of nutrient cycling on other Eurasian shelves (Tuerena, Hopkins, Ganeshram, et al., 2021). We propose a separate removal term for Arctic shelves based on estimates from the Laptev Sea. Productive Arctic shelves account for 39% of the total Arctic Ocean area (Jakobsson, 2002), leading to adjusted fluxes of 0.10–0.18 TmolSi/yr for opal burial in the open Arctic Ocean.

The net burial of Si is approximated from the removal of DSi and the benthic efflux measured by Sun et al. (2021). This approximation is used as the shelf has a shallow water column and fast sedimentation rates, which should lower the exposure time of opal for dissolution in the water column and at the sediment interface (Nelson et al., 1995). We estimated in this study that 55% ± 14% of DSi from riverine origins is removed on the Laptev Sea shelf. Extrapolating this to pan-Arctic river fluxes, we estimate an additional net shelf removal of DSi of 0.24 TmolSi/yr. As the source of DSi from rivers is isotopically lighter than marine-sourced DSi, the isotopic signature of opal buried on shelves ($\delta^{30}Si\text{-}BSiO_2$) from terrestrial origins is estimated using the Rayleigh model fractionation for opal described in Varela et al. (2004):

$$\delta^{30}Si - bSiO_2 = \delta^{30}Si(OH)_{4\text{-initial}} - 30_{\varepsilon}((f \ln f)/(1-f))$$

where $\delta^{30}Si(OH)_{4\text{-initial}}$ is the $\delta^{30}Si(OH)_4$ in surface waters prior to utilization, here +1.30‰ for riverine-sourced DSi. Using a biological fractionation factor of −1.07 as per Section 4.3 and a range of fraction of DSi remaining (0.45 ± 0.14 as per Section 4.3), we calculate a $\delta^{30}Si\text{-}BSiO_2$ of +0.60‰ ± 0.08‰. Ward et al. (2022b) found evidence of isotopically light opal in the BS under Arctic water influence (+0.82‰). Both our estimates and Ward et al.'s (2022b)'s findings are substantially lighter than the $\delta^{30}Si\text{-}BSiO_2$ measured in the Canadian Arctic (Giesbrecht et al., 2022; Varela et al., 2016) and the BS Opening under the influence of AW (Ward et al., 2022b). This potentially reflects the formation of opal from isotopically lighter DSi sources (namely riverine), and its subsequent burial into the sediments in freshwater influenced shelves.

From the inflow and removal terms described above, the $\delta^{30}Si(OH)_4$ of outflowing waters from the Arctic Ocean can be approximated using isotopic mass-balance and assuming steady-state:

$$F_{\text{outflow}} = F_{\text{inflow}} - F_{\text{removal}}$$

$$\delta^{30}Si(OH)_{4\text{-inflow}} = f_{\text{removal}}\ \delta^{30}Si(OH)_{4\text{-removed}} + (1 - f_{\text{removal}})\ \delta^{30}Si(OH)_{4\text{-outflow}}$$

Rearranging for $\delta^{30}Si(OH)_{4\text{-outflow}}$:

$$\mathrm{Si(OH)}_{\text{4-outflow}} = \frac{\delta^{30}\mathrm{Si(OH)}_{\text{4-inflow}} - f_{\text{removal}}\,\delta^{30}\mathrm{Si(OH)}_{\text{4-removed}}}{(1 - f_{\text{removal}})}$$

where F are the fluxes of Si in Tmol/yr, $f_{\text{removal}} = F_{\text{removal}}/F_{\text{inflow}}$ (here 0.38 and 2.37 TmolSi/yr respectively, Table 1), $\delta^{30}\mathrm{Si(OH)}_{\text{4-inflow}}$ is the flux-weighted isotopic signature of inputs (inflow + rivers, 1.64‰) and $\delta^{30}\mathrm{Si}_{\text{removed}} = 0.81‰$, calculated as the flux-weighted isotopic signature of Si removal processes from both the shelf and open ocean. The above equations lead to a predicted outflow of 1.99 TmolSi/yr with an isotopic signature of 1.80‰ ± 0.12‰, based on the ranges provided in Table 1. Using the mean $\delta^{30}\mathrm{Si\text{-}BSiO_2}$ of +0.60‰, modeled shelf burial of isotopically light opal contributes to an isotopic shift of around 0.1‰.

Extrapolating the net removal of nutrients to productive Eurasian shelves helps to close the isotope mass balance of the Arctic Ocean and reproduces well the observed outflowing isotopic signature of the Arctic Ocean (mass-weighted modeled $\delta^{30}\mathrm{Si(OH)_4} = +1.80‰ \pm 0.12‰$, Table 1). The output modeled $\delta^{30}\mathrm{Si(OH)_4}$ is sensitive to the isotopic signature of riverine DSi, which needs to be further constrained through seasonal and annual observations of major Arctic rivers to improve the Arctic Si budget. Our modeled budget simplifies internal cycling processes and ignores potential additional sources of isotopically light DSi from hydrothermal vents (Edmonds et al., 2003; Liguori et al., 2020) and lithogenic sources (Ward et al., 2022b). This could explain the underestimation of the DSi outflow flux by 0.44 TmolSi/yr relative to the observations from Torres-Valdes et al. (2013). Nonetheless, this exercise highlights the sensitivity of the Arctic DSi budget to biological processes, highlighting the role of the Arctic shelf silica pump in elevating the isotopic signature of Arctic DSi, as proposed by Brzezinski et al. (2021), as well as regulating export out to the Atlantic Ocean.

4.5. Future Implications and Limitations

Climate change is significantly affecting the Arctic Ocean and its shallow coastal shelves. Considering its connection to surrounding land, the Arctic Ocean is particularly sensitive to changes in its freshwater budget and terrigenous supply of nutrients (Macdonald et al., 2015). Discharge from Eurasian rivers is increasing (Mcclelland et al., 2006), permafrost thaw and degradation is increasing nutrient fluxes to the coast (Frey & McClelland, 2009; Frey et al., 2007; Zhang et al., 2021), sea-ice cover is decreasing (Notz & Stroeve, 2016) and primary productivity in the Eurasian Arctic is increasing (Frey et al., 2018). These changes have knock-on impacts on phytoplankton dynamics in the Arctic Ocean (Ardyna & Arrigo, 2020) and the prevalence of diatoms is changing (Blais et al., 2017). Changes in the flux and stoichiometry of nutrients delivered to Arctic shelves will impact primary productivity locally but also change nutrient budgets and the export of DSi out of the Arctic Ocean (Torres-Valdés et al., 2013).

We still observe a discrepancy between the predicted and measured DSi at outflow gateways. This can be partially linked to uncertainty within the measurement of fluxes or missing sources of DSi to the Arctic Ocean. Among these suggested sources are hydrothermal vents and lithogenic silica from the benthos (Edmonds et al., 2003; Liguori et al., 2020; Ward et al., 2022b). Kipp et al. (2018) have observed increased fluxes of shelf-derived materials from sediment-exchange, which can significantly change the supply and balance of nutrients on Arctic shelves and impact burial of DSi. Lithogenic supply of DSi could become increasingly important in the future Arctic Ocean, highlighting the importance of further constraining this flux on a basin-wide scale (Ward et al., 2022b).

Nonetheless, the DSi and $\delta^{30}\mathrm{Si(OH)_4}$ isotope budget of the Arctic Ocean shows that biological cycling plays a key role for the burial of opal and export of DSi in the Arctic Ocean. The Arctic shelf silica pump is currently limited by nitrogen. Laukert et al. (2022) speculates that weakening stratification on Eurasian shelves will increase DSi drawdown and reduce DSi export into the TPD. In this view, increased vertical mixing and the supply of marine N fuel diatom production and burial over the shelves. However, it ignores the fact that any increase in productivity over the shelf will also fuel N removal by denitrification as this process is shown to exacerbate organic matter fluxes to sediments (Chang & Devol, 2009; Tuerena, Hopkins, Buchanan, et al., 2021; Tuerena, Mahaffey, Henley, et al., 2021). In addition, increasing riverine discharge and permafrost degradation is likely to increase the export of major nutrients (Zhang et al., 2021). Therefore, it is likely that mixing and riverine input will enhance denitrification in the Eurasian shelf and acerbate N limitation, allowing a smaller proportion of the riverine DSi flux to be buried on Eurasian shelves. This emphasizes the strong biological controls on the shelf silica pump, and

could in turn lead to an increase in DSi export into the TPD, and lower isotopic signatures. Our mass-balanced isotope budget also shows that the $\delta^{30}Si(OH)_4$ of exported DSi is extremely sensitive to the $\delta^{30}Si$ of biogenic Si removed. To further constrain the DSi budget of the Arctic Ocean, better characterization of $\delta^{30}Si$ of biogenic Si and $^{30}\varepsilon$ is needed, particularly within rivers and on Eurasian shelves. Characterization of removal in the East Siberian Sea would also confirm the suitability of extrapolating removal in the Laptev Sea to the Eurasian shelf.

5. Conclusions

This study presents direct measurements of $\delta^{30}Si(OH)_4$ along the Lena Delta and the Laptev Sea, as well as providing surface measurements along a transect on the Eurasian shelves. A gradual increase in DSi, DSi:N ratio and enrichment is found from West to East in the surface waters of the Eurasian shelf. This is attributed to nutrient input from rivers, and partial utilization of DSi and subsequent burial of isotopically light $\delta^{30}Si$ in the shelf sediments.

Nitrogen was found to be strongly depleted on the Laptev Sea shelf, limiting the uptake of DSi. Through heavy silicon isotopic signatures, we trace the partial uptake signal of shelf waters feeding over the continental slope to the TPD, documenting the export of excess riverine DSi to the Arctic Ocean. From isotopic measurements, it is estimated that >50% of DSi from riverine inputs is removed within the Lena River delta and on the Laptev Sea shelf, leading to an export of 2.5 ± 0.8 kmol/s of riverine DSi through the TPD. This highlights the role of Eurasian rivers in supplying nutrients to the Arctic Ocean and the importance of shelves which modify nutrient stoichiometry on Arctic shelves.

An updated isotopic budget of the Arctic Ocean displays the importance of biological processes in controlling DSi export and enriching the $\delta^{30}Si(OH)_4$ of outflowing water masses from the Arctic Ocean. The study highlights the role of nitrogen limitation in the shallow Arctic shelves in determining the DSi fluxes, which are highly sensitive to ongoing climate change. As a consequence of changing biogeochemical cycles in the Arctic Ocean, it is envisioned that changes in the DSi export out of the Arctic will increase and lighter $\delta^{30}Si(OH)_4$ signatures of the Arctic Ocean are expected in the near-future.

Data Availability Statement

Maps and figures were produced using Ocean Data View. All data presented in this study are available from the PANGAEA data set by Debyser et al. (2024), https://doi.org/10.1594/PANGAEA.965315. This data set has also been included in Data Set S1.

Acknowledgments
First, we thank one anonymous reviewer and Greg de Souza for their insightful and detailed comments, which have improved this work. We thank the crew and participants of the 73rd expedition of R/V *Akademik Mstislav Keldysh* (AMK73) for their support in planning and sampling of this project, particularly Adam Francis for sample collection. We also thank Sharon McNeil for the DON measurements at SAMS. This work was supported by a Natural Environment Research Council (NERC) Doctoral Training Partnership Grant (NE/L002558/1) and from the ARISE project NE/P006310/1 awarded to Prof. Raja S. Ganeshram, as part of the Changing Arctic ocean programme, jointly funded by the UKRI NERC and the German Federal Ministry of Education and Research (BMBF). The field work was supported by the Russian Science Foundation (Grant 21-77-30001 awarded to Dr. Igor Semiletov). Additional support was from the Ministry of Science and Higher Education of the Russian Federation (Grant "Priority-2030," Tomsk State University). The charter of the R/V *Akademik Mstislav Keldysh* was funded by Grant 021-2021-0010 from the Ministry of Science and Higher Education of the Russian Federation.

References

Aagaard, K., & Carmack, E. C. (1989). The role of sea ice and other fresh water in the Arctic circulation. *Journal of Geophysical Research*, *94*(C10), 14485–14498. https://doi.org/10.1029/jc094ic10p14485

Ardyna, M., & Arrigo, K. R. (2020). Phytoplankton dynamics in a changing Arctic Ocean. *Nature Climate Change*, *10*(10), 892–903. https://doi.org/10.1038/s41558-020-0905-y

Årthun, M., Ingvaldsen, R. B., Smedsrud, L. H., & Schrum, C. (2011). Dense water formation and circulation in the Barents Sea. *Deep Research Part I Oceanographic Research Papers*, *58*(8), 801–817. https://doi.org/10.1016/j.dsr.2011.06.001

Bauch, D., Hölemann, J., Willmes, S., Gröger, M., Novikhin, A., Nikulina, A., et al. (2010). Changes in distribution of brine waters on the Laptev Sea shelf in 2007. *J. Geophys. Res. Ocean.*, *115*(11), 1–11. https://doi.org/10.1029/2010JC006249

Bauch, D., Schlosser, P., & Fairbanks, R. G. (1995). The distribution of $d^{18}O$ in the Arctic Ocean: Implications for the freshwater balance of the halocline and the sources of deep and bottom waters. *Reports on Polar Research*, *159*(95), 5–143.

Blais, M., Ardyna, M., Gosselin, M., Dumont, D., Bélanger, S., Tremblay, J. É., et al. (2017). Contrasting interannual changes in phytoplankton productivity and community structure in the coastal Canadian Arctic Ocean. *Limnology & Oceanography*, *62*(6), 2480–2497. https://doi.org/10.1002/lno.10581

Brzezinski, M. A. (1985). The Si:C:N ratio of marine diatoms: Interspecific variability and the effect of some environmental variables. *Journal of Phycology*, *21*(3), 347–357. https://doi.org/10.1111/j.0022-3646.1985.00347.x

Brzezinski, M. A., Closset, I., Jones, J. L., de Souza, G. F., & Maden, C. (2021). New constraints on the physical and biological controls on the silicon isotopic composition of the Arctic Ocean. *Frontiers in Marine Science*, *8*(August). https://doi.org/10.3389/fmars.2021.699762

Brzezinski, M. A., & Jones, J. L. (2015). Coupling of the distribution of silicon isotopes to the meridional overturning circulation of the North Atlantic Ocean. *Deep-Sea Research Part II Topical Studies in Oceanography*, *116*, 79–88. https://doi.org/10.1016/j.dsr2.2014.11.015

Brzezinski, M. A., Jones, J. L., Barbara, S., Bidle, K. D., & Azam, F. (2003). The balance between silica production and silica dissolution in the sea: Insights from Monterey Bay, California, applied to the global data set. *Limnology & Oceanography*, *48*(5), 1846–1854. https://doi.org/10.4319/lo.2003.48.5.1846

Carey, J. C., Gewirtzman, J., Johnston, S. E., Kurtz, A., Tang, J., Vieillard, A. M., & Spencer, R. G. M. (2020). Arctic River dissolved and biogenic silicon exports—Current conditions and future changes with warming. *Global Biogeochemical Cycles*, *34*(3), no. https://doi.org/10.1029/2019GB006308

Chang, B. X., & Devol, A. H. (2009). Seasonal and spatial patterns of sedimentary denitrification rates in the Chukchi sea. *Deep. Res. Part II Top. Stud. Oceanogr.*, *56*(17), 1339–1350. https://doi.org/10.1016/j.dsr2.2008.10.024

Charette, M. A., Kipp, L. E., Jensen, L. T., Dabrowski, J. S., Whitmore, L. M., Fitzsimmons, J. N., et al. (2020). The transpolar Drift as a source of riverine and shelf-derived trace elements to the central Arctic Ocean. *Journal of Geophysical Research Oceans*, *125*(5), 1–34. https://doi.org/10.1029/2019JC015920

Cremer, H. (1999). Distribution patterns of diatom surface sediment assemblages in the Laptev Sea (Arctic Ocean). *Marine Micropaleontology*, *38*(1), 39–67. https://doi.org/10.1016/S0377-8398(99)00037-7

Debyser, M. C. F. (2023). *Nutrient cycling in the Arctic and subarctic oceans: A stable isotope study. PhD thesis*. The University of Edinburgh.

Debyser, M. C. F., Pichevin, L., Ganeshram, R. S., & Semiletov, I. P. (2024). Stable dissolved silicon isotopes measured on CTD and underway samples during AMK73 in the Laptev Sea [Dataset]. *PANGAEA*. https://doi.org/10.1594/PANGAEA.965315

Debyser, M. C. F., Pichevin, L., Tuerena, R. E., Dodd, P. A., Doncila, A., & Ganeshram, R. S. (2022). Tracing the role of arctic shelf processes in Si and N cycling and export through the Fram Strait: Insights from combined silicon and nitrate isotopes. *Biogeosciences*, *19*(23), 5499–5530. https://doi.org/10.5194/bg-19-5499-2022

De La Rocha, C. L., Brzezinski, M. A., & Deniro, M. J. (2000). A first look at the distribution of the stable isotopes of silicon in natural waters. *Geochimica et Cosmochimica Acta*, *64*(14), 2467–2477. https://doi.org/10.1016/s0016-7037(00)00373-2

Dittmar, T., & Kattner, G. (2003). The biogeochemistry of the river and shelf ecosystem of the Arctic Ocean: A review. *Marine Chemistry*, *83*(3–4), 103–120. https://doi.org/10.1016/S0304-4203(03)00105-1

Edmonds, H. N., Michael, P. J., Baker, E. T., Connelly, D. P., Snow, J. E., Langmuir, C. H., et al. (2003). Discovery of abundant hydrothermal venting on the ultraslow-spreading Gakkel ridge in the Arctic Ocean. *Nature*, *421*(6920), 252–256. https://doi.org/10.1038/nature01351

Fahl, K., Cremer, H., Erlenkeuser, H., Hanssen, H., Hölemann, J., Kassens, H., et al. (1999). Sources and pathways of organic carbon in the modern Laptev Sea (Arctic Ocean): Implications from biological, geochemical and geological data. *Polarforschung*, *69*(1–3), 193–205.

Francis, A., Ganeshram, R. S., Tuerena, R. E., Spencer, R. G. M., Holmes, R. M., Rodgers, J. A., & Mahaffey, C. (2023). Permafrost degradation and nitrogen cycling in arctic rivers: Insights from stable nitrogen isotope studies. *Biogeosciences*, *20*(2), 365–382. https://doi.org/10.5194/bg-20-365-2023

Frey, K. E., Comiso, J. C., Cooper, L. W., Eisner, L. B., Gradinger, R. R., Grebmeier, J. M., & Tremblay, J. E. (2018). Arctic Ocean primary productivity, Arct. Rep. Card Updat. 2011 (pp. 1–17). Retrieved from http://www.arctic.noaa.gov/report11/primary_productivity.html

Frey, K. E., Comiso, J. C., Cooper, L. W., Grebmeier, J. M., & Stock, L. V. (2021). Arctic Ocean primary productivity: The response of marine algae to climate warming and sea ice decline, NOAA Arct. Rep. Card 2021, (21–07) (pp. 1–12). Retrieved from https://repository.library.noaa.gov/view/noaa/27905

Frey, K. E., & McClelland, J. W. (2009). Impacts of permafrost degradation on arctic river biogeochemistry. *Hydrological Processes*, *23*(1), 169–182. https://doi.org/10.1002/hyp.7196

Frey, K. E., McClelland, J. W., Holmes, R. M., & Smith, L. G. (2007). Impacts of climate warming and permafrost thaw on the riverine transport of nitrogen and phosphorus to the Kara Sea. *Journal of Geophysical Research*, *112*(4), 1–10. https://doi.org/10.1029/2006JG000369

Fripiat, F., Cardinal, D., Tison, J. L., Worby, A., & André, L. (2007). Diatom-induced silicon isotopic fractionation in Antarctic sea ice. *Journal of Geophysical Research*, *112*(2). https://doi.org/10.1029/2006JG000244

Fripiat, F., Cavagna, A. J., Dehairs, F., Speich, S., André, L., & Cardinal, D. (2011). Silicon pool dynamics and biogenic silica export in the Southern Ocean inferred from Si-isotopes. *Ocean Science*, *7*(5), 533–547. https://doi.org/10.5194/os-7-533-2011

Fripiat, F., Cavagna, A. J., Savoye, N., Dehairs, F., André, L., & Cardinal, D. (2011). Isotopic constraints on the Si-biogeochemical cycle of the Antarctic zone in the Kerguelen area (KEOPS). *Marine Chemistry*, *123*(1–4), 11–22. https://doi.org/10.1016/j.marchem.2010.08.005

Fripiat, F., Declercq, M., Sapart, C. J., Anderson, L. G., Bruechert, V., Deman, F., et al. (2018). Influence of the bordering shelves on nutrient distribution in the Arctic halocline inferred from water column nitrate isotopes. *Limnology & Oceanography*, *63*(5), 2154–2170. https://doi.org/10.1002/lno.10930

Fripiat, F., Tison, J. L., André, L., Notz, D., & Delille, B. (2014). Biogenic silica recycling in sea ice inferred from Si-isotopes: Constraints from Arctic winter first-year sea ice. *Biogeochemistry*, *119*(1–3), 25–33. https://doi.org/10.1007/s10533-013-9911-8

Georg, R. B., Reynolds, B. C., Frank, M., & Halliday, A. N. (2006). New sample preparation techniques for the determination of Si isotopic compositions using MC-ICPMS. *Chemical Geology*, *235*(1–2), 95–104. https://doi.org/10.1016/j.chemgeo.2006.06.006

Giesbrecht, K. E. (2019). Biogenic silica dynamics of Arctic marine ecosystems.

Giesbrecht, K. E., Varela, D. E., Souza, G. F., & Maden, C. (2022). Natural variations in dissolved silicon isotopes across the Arctic Ocean from the Pacific to the Atlantic. *Global Biogeochemical Cycles*, *36*(5), 1–23. https://doi.org/10.1029/2021gb007107

Grasse, P., Brzezinski, M. A., Cardinal, D., Souza, G. F. D., Estrade, N., François, R., et al. (2017). GEOTRACES inter-calibration of the stable silicon isotope composition of dissolved silicic acid in seawater. *Journal of Analytical Atomic Spectrometry*, *32*(3), 562–578. https://doi.org/10.1039/c6ja00302h

Gruber, N., & Sarmiento, J. L. (1997). Global patterns of marine nitrogen fixation and denitrification. *Global Biogeochemical Cycles*, *11*(2), 235–266. https://doi.org/10.1029/97gb00077

Holmes, R. M., Mcclelland, J. W., Peterson, B. J., Tank, S. E., Bulygina, E., Eglinton, T. I., et al. (2012). Seasonal and annual fluxes of nutrients and organic matter from large rivers to the Arctic Ocean and surrounding seas. *Estuaries and Coasts*, *35*(2), 369–382. https://doi.org/10.1007/s12237-011-9386-6

Holmes, R. M., McClelland, J. W., Tank, S. E., Spencer, R. G. M., & Shiklomanov, A. I. (2019). Arctic Great rivers observatory [Dataset]. *Waterquality, Version 20190904*. Retrieved from https://arcticgreatrivers.org/data/

Jakobsson, M. (2002). Hypsometry and volume of the Arctic Ocean and its constituent seas. *Geochemistry, Geophysics, Geosystems*, *3*(5), 1–18. https://doi.org/10.1029/2001gc000302

Janout, M. A., Hölemann, J., Laukert, G., Smirnov, A., Krumpen, T., Bauch, D., & Timokhov, L. (2020). On the variability of stratification in the freshwater-influenced Laptev Sea region. *Frontiers in Marine Science*, *7*(September), 1–17. https://doi.org/10.3389/fmars.2020.543489

Karcher, M. J., & Oberhuber, J. M. (2002). Pathways and modification of the upper and intermediate waters of the Arctic Ocean. *Journal of Geophysical Research*, *107*(C6), 1–13. https://doi.org/10.1029/2000jc000530

Karl, D. M., & Tien, G. (1992). MAGIC: A sensitive and precise method for measuring dissolved phosphorus in aquatic environments. *Limnology & Oceanography*, *37*(1), 105–116. https://doi.org/10.4319/lo.1992.37.1.0105

Kipp, L. E., Charette, M. A., Moore, W. S., Henderson, P. B., & Rigor, I. G. (2018). Increased fluxes of shelf-derived materials to the central Arctic ocean. *Science Advances*, *4*(1), 1–10. https://doi.org/10.1126/sciadv.aao1302

Kostyleva, A. V., Polukhin, A. A., & Stepanova, S. V. (2020). Hydrochemical structural patterns of the Lena River–Laptev Sea mixing zone in the Autumn period. *Oceanology*, *60*(6), 735–741. https://doi.org/10.1134/S0001437020060053

Krause, J. W., Schulz, I. K., Rowe, K. A., Dobbins, W., Winding, M. H. S., Sejr, M. K., et al. (2019). Silicic acid limitation drives bloom termination and potential carbon sequestration in an Arctic bloom. *Scientific Reports*, *9*(1), 1–11. https://doi.org/10.1038/s41598-019-44587-4

Laukert, G., Grasse, P., Novikhin, A., Povazhnyi, V., Doering, K., Hölemann, J., et al. (2022). Nutrient and silicon isotope dynamics in the Laptev Sea and implications for nutrient availability in the transpolar Drift. *Global Biogeochemical Cycles*, *36*(9), e2022GB007316. https://doi.org/10.1029/2022gb007316

Le Fouest, V., Babin, M., & Tremblay, J. E. (2013). The fate of riverine nutrients on Arctic shelves. *Biogeosciences*, *10*(6), 3661–3677. https://doi.org/10.5194/bg-10-3661-2013

Létolle, R., Martin, J. M., Thomas, A. J., Gordeev, V. V., Gusarova, S., & Sidorov, I. S. (1993). ^{18}O abundance and dissolved silicate in the Lena delta and Laptev Sea (Russia). *Marine Chemistry*, *43*(1–4), 47–64. https://doi.org/10.1016/0304-4203(93)90215-A

Letscher, R. T., Hansell, D. A., Kadko, D., & Bates, N. R. (2013). Dissolved organic nitrogen dynamics in the Arctic Ocean. *Marine Chemistry*, *148*, 1–9. https://doi.org/10.1016/j.marchem.2012.10.002

Liguori, B. T. P., Ehlert, C., Nöthig, E. M., van Ooijen, J. C., & Pahnke, K. (2021). The transpolar drift influence on the Arctic Ocean silicon cycle. *Journal of Geophysical Research Oceans*, *126*(11), e2021JC017352. https://doi.org/10.1029/2021JC017352

Liguori, B. T. P., Ehlert, C., & Pahnke, K. (2020). The influence of water mass mixing and particle dissolution on the silicon cycle in the central Arctic Ocean. *Frontiers in Marine Science*, *7*(April), 1–16. https://doi.org/10.3389/fmars.2020.00202

Macdonald, R. W., Anderson, L. G., Christensen, J. P., Miller, L., Semiletov, I. P., & Stein, R. (2010). The Arctic Ocean. In K. K. Liu (Ed.) *Carbon and nutrient fluxes in continental margins* (pp. 292–303). Springer-Verlag.

Macdonald, R. W., Kuzyk, Z. A., & Johannessen, S. C. (2015). It is not just about the ice: A geochemical perspective on the changing Arctic Ocean. *Journal of Environmental Studied Sciences*, *5*(3), 288–301. https://doi.org/10.1007/s13412-015-0302-4

Mammone, K. A. (1998). Sediment provenance and transport on the Siberian Arctic shelf. Master thesis.

März, C., Meinhardt, A. K., Schnetger, B., & Brumsack, H. J. (2015). Silica diagenesis and benthic fluxes in the Arctic Ocean. *Marine Chemistry*, *171*, 1–9. https://doi.org/10.1016/j.marchem.2015.02.003

Mavromatis, V., Rinder, T., Prokushkin, A. S., Pokrovsky, O. S., Korets, M. A., Chmeleff, J., & Oelkers, E. H. (2016). The effect of permafrost, vegetation, and lithology on Mg and Si isotope composition of the Yenisey River and its tributaries at the end of the spring flood. *Geochimica et Cosmochimica Acta*, *191*, 32–46. https://doi.org/10.1016/j.gca.2016.07.003

Mcclelland, J. W., De, S. J., Peterson, B. J., Holmes, R. M., & Wood, E. F. (2006). A pan-arctic evaluation of changes in river discharge during the latter half of the 20th century. *Geophysical Research Letters*, *33*, 2–5. https://doi.org/10.1029/2006GL025753

McClelland, J. W., Holmes, R. M., Dunton, K. H., & Macdonald, R. W. (2012). The Arctic Ocean estuary. *Estuaries and Coasts*, *35*(2), 353–368. https://doi.org/10.1007/s12237-010-9357-3

Nelson, D. M., Tréguer, P., Brzezinski, M. A., Leynaert, A., & Quéguiner, B. (1995). Production and dissolution of biogenic silica in the ocean: Revised global estimates, comparison with regional data and relationship to biogenic sedimentation. *Global Biogeochemical Cycles*, *9*(3), 359–372. https://doi.org/10.1029/95gb01070

Notz, D., & Stroeve, J. (2016). Observed Arctic sea-ice loss directly follows anthropogenic CO_2 emission. *Science*, *354*(6313), 747–750. https://doi.org/10.1126/science.aag2345

Nürnberg, D., Stein, R., Polyakova, Y., & Pivovoarov, S. V. (1997). *Biogenic opal in shallow Eurasian shelf sediments in relation to the pelagic Arctic Ocean environment*. Mitteilungen zur Kieler Polarforsch.

Osadchiev, A. A., Pisareva, M. N., Spivak, E. A., Shchuka, S. A., & Semiletov, I. P. (2020). Freshwater transport between the Kara, Laptev, and East-Siberian seas. *Scientific Reports*, *10*(1), 13041. https://doi.org/10.1038/s41598-020-70096-w

Pavlov, V. K., Timokhov, L. A., Baskakov, G. A., Kulakov, M. Y., Kurazhov, V. K., Pavlov, P. V., et al. (1996). Hydrometeorological regime of the Kara, Laptev, and East-Siberian seas. In *Technical Memoranda APL-UW TM, (January)* (pp. 1–96).

Pokrovsky, O. S., Reynolds, B. C., Prokushkin, A. S., Schott, J., & Viers, J. (2013). Silicon isotope variations in Central Siberian rivers during basalt weathering in permafrost-dominated larch forests. *Chemical Geology*, *355*, 103–116. https://doi.org/10.1016/j.chemgeo.2013.07.016

Reynolds, B. C., Aggarwal, J., Andre, L., Georg, R. B., Beucher, C., Brzezinski, M. A., et al. (2007). An inter-laboratory comparison of Si isotope reference materials. *Journal of Analytical Atomic Spectrometry*, *22*(5), 561–568. https://doi.org/10.1039/b616755a

Reynolds, B. C., Frank, M., & Halliday, A. N. (2006). Silicon isotope fractionation during nutrient utilization in the North Pacific. *Earth and Planetary Science Letters*, *244*(1–2), 431–443. https://doi.org/10.1016/j.epsl.2006.02.002

Rudels, B., Jones, E. P., Schauer, U., & Eriksson, P. (2004). Atlantic sources of the Arctic Ocean surface and halocline waters. *Polar Research*, *23*(2), 181–208. https://doi.org/10.1111/j.1751-8369.2004.tb00007.x

Sakshaug, E. (2004). Primary and secondary production in the Arctic seas. In *Organic carbon cycle Arctic Ocean* (pp. 57–81). https://doi.org/10.1007/978-3-642-18912-8_3

Sarmiento, J. L., Gruber, N., Brzezinski, M. A., & Dunne, J. P. (2004). High-latitude controls of thermocline nutrients and low latitude biological productivity. *Nature*, *427*(January), 56–60. https://doi.org/10.1038/nature02204.1

Semiletov, I. P., Dudarev, O., Luchin, V., Shin, K.-H., & Tanaka, N. (2005). The East-Siberian Sea as a transition zone between Pacific-derived waters and Artic shelf waters. *Geophysical Research Letters*, *32*, L10614. https://doi.org/10.1029/2005gl022490

Semiletov, I. P., Savelieva, N. I., Weller, G. E., Pipko, I. I., Pugach, S. P., Gukov, A. Y., & Vasilevskaya, L. N. (2000). The dispersion of Siberian river flows into coastal waters: Meteorological, hydrological and hydrochemical aspects. In E. Lewis, E. P. Jones, P. Lemke, T. D. Prowse, & P. Wadhams (Eds.), *The freshwater budget of the Arctic Ocean* (pp. 323–366). Springer.

Simpson, K. G., Tremblay, J. É., Gratton, Y., & Price, N. M. (2008). An annual study of inorganic and organic nitrogen and phosphorus and silicic acid in the southeastern Beaufort Sea. *Journal of Geophysical Research Oceans*, *113*(7), 1–16. https://doi.org/10.1029/2007JC004462

Souza, G. F. D., Reynolds, B. C., Rickli, J., Frank, M., Saito, M. A., Gerringa, L. J. A., & Bourdon, B. (2012). Southern Ocean control of silicon stable isotope distribution in the deep Atlantic Ocean. *Global Biogeochemical Cycles*, *26*(2), 1–13. https://doi.org/10.1029/2011gb004141

Spivak, E. A., Osadchiev, A. A., & Semiletov, I. P. (2021). Structure and variability of the Lena River plume in the South-Eastern part of the Laptev Sea. *Oceanology*, *61*(6), 839–849. https://doi.org/10.1134/S000143702106014X

Stedmon, C. A., Amon, R. M. W., Rinehart, A. J., & Walker, S. A. (2011). The supply and characteristics of colored dissolved organic matter (CDOM) in the Arctic Ocean: Pan arctic trends and differences. *Marine Chemistry*, *124*(1–4), 108–118. https://doi.org/10.1016/j.marchem.2010.12.007

Sun, X., Humborg, C., Mörth, C. M., & Brüchert, V. (2021). The importance of benthic nutrient fluxes in supporting primary production in the Laptev and East Siberian shelf seas. *Global Biogeochemical Cycles*, *35*(7), e2020GB006849. https://doi.org/10.1029/2020GB006849

Sun, X., Mörth, C. M., Porcelli, D., Kutscher, L., Hirst, C., Murphy, M. J., et al. (2018). Stable silicon isotopic compositions of the Lena River and its tributaries: Implications for silicon delivery to the Arctic Ocean. *Geochimica et Cosmochimica Acta*, *241*, 120–133. https://doi.org/10.1016/j.gca.2018.08.044

Sundfjord, A., Fer, I., Kasajima, Y., & Svendsen, H. (2007). Observations of turbulent mixing and hydrography in the marginal ice zone of the Barents Sea. *Journal of Geophysical Research Oceans*, *112*(5), 1–23. https://doi.org/10.1029/2006JC003524

Terhaar, J., Lauerwald, R., Regnier, P., Gruber, N., & Bopp, L. (2021). Around one third of current Arctic Ocean primary production sustained by rivers and coastal erosion. *Nature Communications*, *12*(1), 1–10. https://doi.org/10.1038/s41467-020-20470-z

Thibodeau, B., Bauch, D., & Voss, M. (2017). Nitrogen dynamic in Eurasian coastal Arctic ecosystem: Insight from nitrogen isotope. *Global Biogeochemical Cycles*, *31*(5), 836–849. https://doi.org/10.1002/2016GB005593

Torres-Valdés, S., Tsubouchi, T., Bacon, S., Naveira-Garabato, A. C., Sanders, R., McLaughlin, F. A., et al. (2013). Export of nutrients from the Arctic Ocean. *Journal of Geophysical Research Oceans*, *118*(4), 1625–1644. https://doi.org/10.1002/jgrc.20063

Tréguer, P. J., Sutton, J. N., Brzezinski, M., Charette, M. A., Devries, T., Dutkiewicz, S., et al. (2021). Reviews and syntheses: The biogeochemical cycle of silicon in the modern ocean. *Biogeosciences*, *18*(4), 1269–1289. https://doi.org/10.5194/bg-18-1269-2021

Tremblay, J. É., Simpson, K., Martin, J., Miller, L., Gratton, Y., Barber, D., & Price, N. M. (2008). Vertical stability and the annual dynamics of nutrients and chlorophyll fluorescence in the coastal, southeast Beaufort Sea. *Journal of Geophysical Research Oceans*, *113*(7), 1–14. https://doi.org/10.1029/2007JC004547

Tuerena, R. E., Hopkins, J., Buchanan, P. J., Ganeshram, R. S., Norman, L., von Appen, W., et al. (2021). An Arctic strait of two halves: The changing dynamics of nutrient uptake and limitation across the Fram Strait. *Global Biogeochemical Cycles*, *35*(9), e2021GB006961. https://doi.org/10.1029/2021gb006961

Tuerena, R. E., Hopkins, J., Ganeshram, R., Norman, L., De La Vega, C., Jeffreys, R., & Mahaffey, C. (2021). Nitrate assimilation and regeneration in the Barents Sea: Insights from nitrate isotopes. *Biogeosciences*, *18*(2), 637–653. https://doi.org/10.5194/bg-18-637-2021

Tuerena, R. E., Mahaffey, C., Henley, S. F., de la Vega, C., Norman, L., Brand, T., et al. (2021). Nutrient pathways and their susceptibility to past and future change in the Eurasian Arctic Ocean. *Ambio*, *51*(2), 355–369. https://doi.org/10.1007/s13280-021-01673-0

Varela, D. E., Brzezinski, M., Beucher, C., Jones, J., Giesbrecht, K., Lansard, B., & Mucci, A. (2016). Heavy silicon isotopic composition of silicic acid and biogenic silica in Arctic waters over the Beaufort shelf and the Canada Basin. *Global Biogeochemical Cycles*, *30*(6), 804–824. https://doi.org/10.1002/2015GB005277

Varela, D. E., Pride, C. J., & Brzezinski, M. A. (2004). Biological fractionation of silicon isotopes in Southern Ocean surface waters. *Global Biogeochemical Cycles*, *18*(1), GB1047. https://doi.org/10.1029/2003GB002140

Ward, J. P. J., Hendry, K. R., Arndt, S., Faust, J. C., Freitas, F. S., Henley, F., et al. (2022a). Benthic silicon cycling in the arctic Barents Sea: A reaction-transport model study (pp. 1–34).

Ward, J. P. J., Hendry, K. R., Arndt, S., Faust, J. C., Freitas, F. S., Henley, S. F., et al. (2022b). Stable silicon isotopes uncover a mineralogical control on the benthic silicon cycle in the arctic Barents Sea. *Geochimica et Cosmochimica Acta*, *329*, 206–230. https://doi.org/10.1016/j.gca.2022.05.005

Young, E. D., Galy, A., & Nagahara, H. (2002). Kinetic and equilibrium mass-dependent isotope fractionation laws in nature and their geochemical and cosmochemical significance. *Geochimica et Cosmochimica Acta*, *66*(6), 1095–1104. https://doi.org/10.1016/S0016-7037(01)00832-8

Zhang, S. M., Mu, C. C., Li, Z. L., Dong, W. W., Wang, X. Y., Streletskaya, I., et al. (2021). Export of nutrients and suspended solids from major Arctic rivers and their response to permafrost degradation. *Advances in Climate Change Research*, *12*(4), 466–474. https://doi.org/10.1016/j.accre.2021.06.002